Check for updates

ASME Journal of Engineering for Gas Turbines and Power
Online journal at:
https://asmedigitalcollection.asme.org/gasturbinespower

Working Fluid Selection and Thermodynamic Optimization of the Novel Renewable Energy-Based RESTORE Seasonal Storage Technology

Dario Alfani[1]
Department of Energy,
Politecnico di Milano,
Milano 20156, Italy
e-mail: dario.alfani@polimi.it

Andrea Giostri
Department of Energy,
Politecnico di Milano,
Milano 20156, Italy
e-mail: andrea.giostri@polimi.it

Marco Astolfi
Department of Energy,
Politecnico di Milano,
Milano 20156, Italy
e-mail: marco.astolfi@polimi.it

Seasonal-based energy storage is expected to be one of the main options for the decarbonization of the space heating sector by increasing the renewables dispatchability. Technologies available today are mainly based on hot water and can only partially fulfill the efficiency, energy density and affordability requirements. This work analyzes a novel system based on pumped thermal energy storage (PTES) concept to maximize renewables and waste heat exploitation during summer and make them available during winter. Organic fluid-based cycles are adopted for the heat upgrade during hot season (heat pump (HP)) and to produce electricity and hot water during cold season (power unit (PU)). Upgraded thermal energy drives an endothermic reaction producing dehydrated solid salts, which can be stored for months using inexpensive and high energy density solutions. This paper focuses on thermodynamic cycles design, comparing the performance attainable with several working fluids. Two different configurations are investigated: coupled systems, sharing the fluid and heat exchangers in both operating modes, and decoupled systems. A preliminary economic assessment completes the study, including a sensitivity analysis on electricity and heat prices. Cyclopentane is identified as a promising working fluid for coupled systems, reaching competitive round trip efficiencies (RTEs), maximizing the ratio between performance and HX surfaces, without excessive turbomachinery volume ratios and volumetric flows. Economic analysis shows that solutions with lower efficiency, but also lower capital cost, can achieve competitive payback times (PBT). On the contrary, decoupled systems are less attractive, as they reach slightly higher thermodynamic performance, but require higher capital costs, possibly being of interest only in specific applications.
[DOI: 10.1115/1.4065407]

1 Introduction: Conventional Seasonal Thermal Energy Storage

Residential sector at European level covers 24.6% of final energy consumption, corresponding to around 283.9 Mton per year [1]. The largest share of energy consumption at household level is used for space and water heating, corresponding to around 80% of the total, of which a large fraction is covered by fossil fuels burned in conventional boilers. As a result, the space heating sector releases 843 Mton of CO_2 per year, equivalent to approximately 26.3% of the total energy-related CO_2 emissions at European level [1]. In addition, in Europe, the integration of renewable energy sources in district heating (DH) networks is still limited to around 19.5% [2], mainly due to their unpredictability and lack of dispatchability, while natural gas accounts for 37% of total heat production, followed by coal with 25% [1]. Seasonal thermal energy storage (TES) is widely recognized as a fundamental asset for the decarbonization of the space heating sector allowing to store a large amount of the renewable energy surplus available during summer season to make it available during the winter one, preventing energy curtailment and supporting energy security at European level [3]. Different seasonal energy storage solutions have already been proposed, tested, and in some cases implemented in real DH networks. Among them, the most mature technologies are (i) Aquifer thermal energy storage (ATES) that exploits the availability of a low-depth aquifer having an adequate stratigraphy of the soil and composition as thermal capacity medium [4–6], (ii) Borehole thermal energy storage (BTES) that adopts water or a water-glycol solution flowing in a closed loop through a number of high-density polyethylene vertical U-type pipes allocated in holes filled by grout and drilled in the ground in a grid disposition able to optimize the system effectiveness [7], (iii) Cavern thermal energy storage and water pits, which consist in the use of an insulated underground vessel or 10–15 m deep pools, filled with hot water during summer period and discharged during wintertime. This technology has been

Turbomachinery Technical Conference & Exposition, Hynes Convention Center, June 26–30, 2023. Turbo Expo 2023.
[1]Corresponding author.
Manuscript received February 16, 2024; final manuscript received March 3, 2024; published online May 21, 2024. Editor: Jerzy T. Sawicki.

Copyright © 2024 by ASME; reuse license CC-BY 4.0

Downloaded from http://asmedigitalcollection.asme.org/gasturbinespower/article-pdf/146/10/101013/7343132/gtp_146_10_101013.pdf by Politecnico Di Milano user on 09 July 2024

already adopted for 75,000 m^3 in Denmark [8], and it currently seems to represent the most mature option for large seasonal energy storage as manufacturers claim a maximum thermal efficiency of 90% and a target cost of 30 €/m^3 [9].

All these TES technologies show some intrinsic limits:

- The HTF medium is usually water or a water–glycol mixture with maximum temperatures of 50–70 °C, thus requiring a thermal integration during winter, often from natural gas combustion, unless additional heat pumps, air heating, or floor heating are adopted.
- The modest heat capacity of the materials employed, with values from 1.2 kWh/m^3K for water and 0.3–0.7 kWh/m^3K for soil, depending on the composition, leads to limited energy densities: 60 kWh/m^3 for water pits, 20–30 kWh/m^3 for ATES and only 0.2–0.4 kWh/m^3 for BTES.
- Integration of renewable energies during summer season is limited to solar energy and waste heat with a temperature downgrade down to 50–100 °C or dissipation of electrical renewable energies (PV or wind) to produce warm water.

2 Proposed Technology and Scope of Work

2.1 Pumped Thermal Energy Storage Concept and Proposed Solution Based on Thermochemical Storage. Pumped Thermal Energy Storage is a technology that uses electrical power during the charging phase to store heat at a temperature different from the ambient one and later exploits that heat to improve the performance of the discharging phase. From its general definition, PTES systems conceptually encompass most of the energy storage solutions different from electrochemical energy storage, flywheels, and pumped hydro. For example, it is possible to conceptually classify as PTES semiclosed commercial systems like the adiabatic compressed air energy storage from Hydrostor [10] and the CO_2 battery from EnergyDome [11], where the compression heat is stored at temperatures up to 400–600 °C, and the liquid air energy storage from Highview Power [12], that stores heat at both temperatures higher than the ambient one (from compressors intercoolers) and at cryogenic temperatures. Differently, Carnot battery technologies are based on the adoption of closed thermodynamic cycles in both charging phase (heat pump for heat temperature upgrade) and discharging phase (heat exploitation with a power cycle) and thus they require only the storage of heat, potentially simplifying the system design and operation and reducing the size for seasonal storage. The use of different thermodynamic cycles is proposed in literature and in the market for Carnot batteries: (i) closed gas Brayton cycles are commercialized by Malta Inc. [13] and also studied by Southwest Research Institute [14], (ii) Steam Rankine cycles have been proposed by H2020 CHESTER project [15], (iii) organic rankine cycles (ORC) are investigated by CHESTER [16] and RESTORE H2020 projects [17] while transcritical CO_2 cycles are proposed by Man Energy Solution [18] and Echogen [19]. Additionally, some systems architectures do not adopt a heat pump for the charging cycle preferring to directly dissipate electrical power to the HTF medium, usually air, and eventually to rocks, as proposed by Siemens Gamesa [20], Pintail Power [21], and Enel Green Power in cooperation with Brenmiller Energy [22]. Each thermodynamic system must be then integrated with the thermal energy storage, which can be a sensible heat storage, a latent heat storage adopting a phase change material (ice for low temperature storage, salts and their eutectic mixtures for temperatures up to 700–800 °C [23]), or a thermochemical storage, where the heat is used to support a specific chemical reaction. Latent and thermochemical energy storage are mainly proposed for thermodynamic cycles with a pure working fluid phase transition (i.e., evaporation and condensation of organic fluids or CO_2) while sensible heat is preferable for Brayton cycles, supercritical CO_2, or non-eutectic fluid mixtures, thanks to the better matching of the temperature profiles.

RESTORE H2020 project [17] aims to provide an answer to the limits of currently available seasonal energy storage technologies by proposing a PTES-Carnot battery system based on the integration of nonconventional organic fluid thermodynamic cycles and innovative thermochemical energy storage. Figure 1 depicts the principle of operation: during summer season, the surplus of thermal energy from renewables (solar, geothermal) or waste heat and the off-peak electricity from photovoltaic (PV) and wind are employed for powering a high temperature HP that collects the available heat for working fluid evaporation at around 80–100 °C and releases heat at higher temperature through fluid condensation. High temperature heat is released to a thermochemical reactor where it is used for a specific endothermic dehydration reaction, which produces water and a solid salt B starting from a solid hydrated salt A, according to reaction reported in Eq. (1).

Seasonal energy storage is thus provided by the accumulation of large quantities of solid salts in piles, vessels, or silos, at ambient pressure and temperature like those commonly adopted in food and chemical industry. During winter season, the reaction is reverted, and salt B is hydrated back to salt A releasing the same amount of energy stored during the charging phase to a PU cycle based on ORC technology that produces electricity and releases the heat of condensation to the district heating water

$$A + \Delta h_{\text{react}} \leftrightarrow B + H_2O \tag{1}$$

Main features connected to decarbonization of space heating sector and seasonal thermal storage are the following:

- Capability to exploit both thermal and electrical RES avoiding their curtailment during summer period and providing an efficient heat temperature upgrade thanks to the use of high-temperature heat pumps characterized by a high coefficient of performance (COP).
- Adoption of a seasonal storage solution at ambient pressure and temperature, based on a solid medium characterized by a very high energy density (up to 2 GJ/m^3), limited land occupation, and negligible energy losses.
- High flexibility in providing heat during discharge at different temperature levels by means of a proper tuning of the power cycle condensation temperature.
- Relatively good electrical RTE on seasonal base (>35%), comparable to those achievable with H_2 from electrolysis + fuel cells.
- Water use is limited to winter months where there is a large availability while water can be potentially released after post treatment during summer months.

2.2 Scope of Work and Methodology. This paper aims to select the optimal working fluid for the RESTORE concept by investigating two different system architectures:

- **Decoupled cycles:** two different cycles are designed for the charging (heat pump –HP) and the discharging cycle (power unit – PU). As result, these systems involve not only a high capital cost but also the following advantages: (i) two different

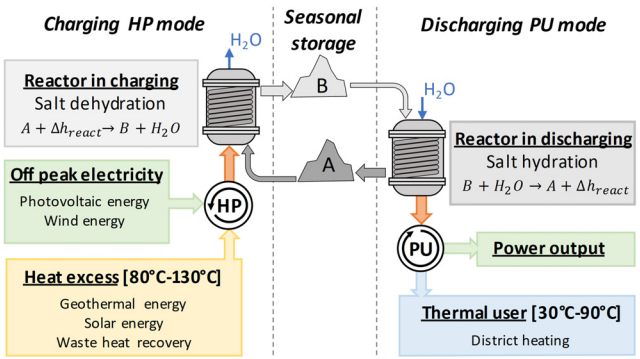

Fig. 1 Overall RESTORE concept seasonal operation

Downloaded from http://asmedigitalcollection.asme.org/gasturbinespower/article-pdf/146/10/101013/7343132/gtp_146_10_101013.pdf by Politecnico Di Milano user on 09 July 2024

working fluids can be selected for the two cycles allowing to reach better thermodynamic performance and (ii) the heat exchangers can be designed for a single operating condition exploiting the most affordable HX architecture for each process (i.e., kettle reboiler for the HP evaporator and shell-and-tube condenser for PU with the organic fluid on shell side and cooling water in tubes).

- **Coupled cycles:** the same heat exchangers are adopted in the charging HP mode and the discharging PU mode. In this case, a single working fluid must be selected, taking into account the different requirements of the two cycles. Moreover, heat exchangers must be sufficiently flexible to be operated in both modes: this is not a relevant issue for the recuperator, while it poses some limits for the low-pressure heat exchanger, which must be able to switch from evaporator (HP) to condenser (PU). For this component, a once-through heat exchanger should be implemented with working fluid flowing in the tubes and water in the shell side. Additionally, coupled cycles can also share the same machine in both modes, namely using a compressor that can be operated reversibly as an expander: volumetric machines (i.e., screw/scroll/piston) can be used in this case, but this option is not investigated in this paper due to the lack of off-design non-dimensional performance maps for these kinds of machines in literature.

Figure 2 represents the scheme of the proposed coupled cycle architecture in both charging and discharging mode. In order to exploit the matching between the isothermal reactor and isothermobaric phase transition in both HP condensation and PU evaporation, the working fluid phase change occurs directly within the reactor, which is thus designed as a coiled stirred reactor. Additional phase separation vessels, not reported in the figure, can be included in order to control throttling valve and turbine admission thermodynamic conditions. The scheme of a decoupled system is conceptually very similar, with the only differences related to the duplication of the heat exchangers, the need of two reactors (or a double coiled one), the compressor and turbine installed on different loops, and the avoidance of three-way valves for the working fluid flow inversion.

Previous studies have already shown the potential of ORC-based PTES systems considering both decoupled and coupled cycles architectures and, in this latter case, scientific literature has mostly focused on small-size systems that allow for the adoption of volumetric machines working as compressors in charge operation and expanders during discharge.

Steger [24] carried out a numerical multi-objective (electrical storage capacity and power-to-power efficiency) Pareto optimization to provide insights on the design and working fluid selection of a reversible HP/ORC system coupled to a latent energy storage. In particular, the authors highlighted the relevance of the working fluid enthalpy of vaporization in the process design, as it directly affects its mass flowrate and thus the investment costs of the system.

Studying a similar system and considering the same working fluids (cyclopentane, R1233zd(E), Novec649, and R365mfc), Eppinger [25] achieved power-to-power efficiencies above 60% for a heat source temperature of 110 °C, adopting both a sensible and latent heat storage for a noncogenerative system. The authors performed several parametric analyses and highlighted that, for most of the investigated cases, R1233zd(E) appeared to be the best choice thanks to the tradeoff between system efficiency and environmental sustainability and safety. However, when considering also latent storage solutions, cyclopentane achieved the highest power-to-power efficiency.

Limiting their analysis to reversible systems coupled to a sensible heat storage, Dumont [26] developed a set of performance maps considering different combinations of working fluid, waste heat temperature (50–90 °C), storage temperature glide (5–15 °C), and ambient temperature (0–40 °C). The authors identified R1233zd(e), R1234yf, R11, R236ea, and R245fa as the working fluids presenting the best performances.

In the framework of the H2020 CHESTER project, Jockenhöfer [27] investigated a decoupled system adopting butane for both the charging and discharging cycles. The results of the analysis showed that the investigated system can provide a net power ratio of 1.25 if a heat source temperature of 100 °C and a heat sink temperature of 15 °C are available.

A similar system has been studied by Frate [28] investigating 17 working fluid candidates but limiting the analysis to a sensible heat storage. The numerical results showed the possibility to boost the round trip efficiency to values higher than 100% when also exploiting a low-grade heat source. Considering a heat source temperature of 110 °C, R1233zd(E) has been identified as the optimal fluid as it allows to achieve a theoretical maximum RTE of 130%.

This work aims to provide new insights about the ORC potential in PTES solutions focusing on the possibility of the adoption of thermochemical energy storage unlocking the possibility of seasonal storage, a feature that cannot be achieved with both latent and sensible storage solutions due to the high heat loss over months of storage. In addition, this paper focuses on the design of a cogenerative system where both electricity and heat are a valuable output, with relevant impact on the economic feasibility of the technology, an aspect not considered in literature so far since studies are only focused on short-term storage. Finally, from numerical point of view, this work aims at an accurate description of the heat transfer process in the heat exchangers, allowing to calculate the heat transfer surfaces and to evaluate the performance of coupled systems with a higher level of detail, catching the effects related to fluid thermodynamic properties variation when passing from charging to discharging mode.

3 Methodology and Numerical Code Description

The numerical code is implemented in Phyton 3.10 integrating REFPROP 10 [29] for the calculation of the working fluid thermodynamic and transport properties. The solving scheme employed in the numerical model is reported in Fig. 3, and it is discussed in detail in Secs. 3.1 and 3.2 for the charging and discharging cycles, respectively. Figure 4 depicts the thermodynamic cycles in charge and discharge modes in a temperature-specific entropy (T-s) diagram for cyclopentane using the same thermodynamic streams indexing of Fig. 2.

3.1 Charging Mode: Heat Pump Cycle. The solving scheme of the charging mode is reported in Fig. 3 on the left, showing the interconnections between assumptions and thermodynamic streams calculation. Calculation routine starts from the heat pump cycle in charging mode by computing the evaporation and condensation

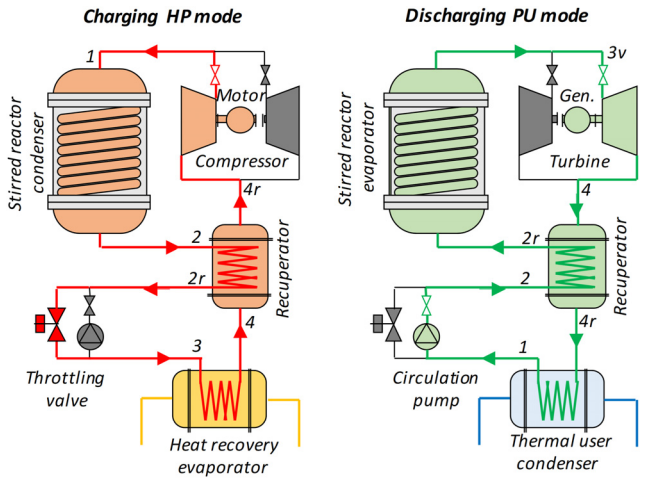

Fig. 2 Coupled cycles configuration scheme adopting reversible heat exchangers

Downloaded from http://asmedigitalcollection.asme.org/gasturbinespower/article-pdf/146/10/101013/7343132/gtp_146_10_101013.pdf by Politecnico Di Milano user on 09 July 2024

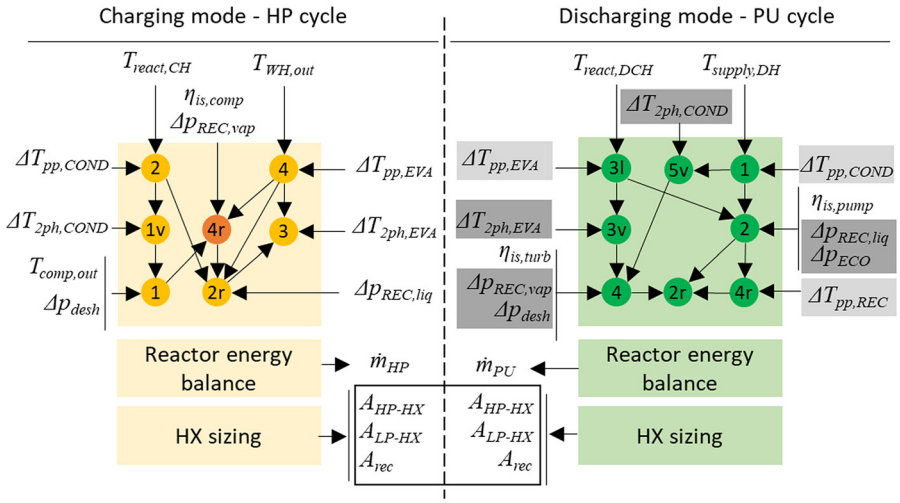

Fig. 3 Solving scheme for the HP (left) and PU cycle (right). For the HP cycle, point 4r requires an iterative calculation. Only for the coupled cycle architecture, parameters in light gray boxes are obtained by matching heat exchangers surfaces, while pressure drops in dark gray boxes are calculated.

temperatures (points 2 and 4) from the outlet temperature of the residual renewable or waste heat ($T_{WH,out}$) and the operating temperature of the chemical reactor in charging mode ($T_{react,CH}$), assuming heat exchangers pinch point temperature differences (ΔT_{pp}) equal to 2 °C. The waste heat source outlet temperature $T_{WH,out}$ is set equal to 80 °C as representative of midtemperature solar energy, geothermal energy, or low temperature waste heat recovery, while the reactor charging temperature $T_{react,CH}$ is set equal to 150 °C according to the preliminary experiments carried out by the Technical University of Wien (TUW), partner of the H2020 RESTORE project, on H_3BO_3-B_2O_3 reaction and other salt hydration and dehydration processes.

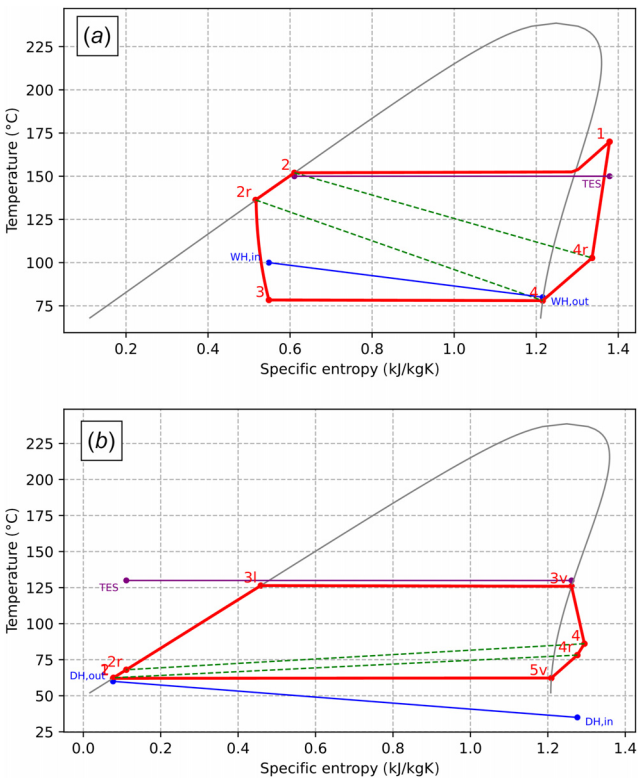

Fig. 4 T-s diagrams for (*a*) charging and (*b*) discharging cycles using cyclopentane in coupled cycle configuration

Saturated vapor condition (point 1_v) is calculated by assuming a fixed pressure drop in phase transition defined as a temperature difference ($\Delta T_{2ph,COND}$) between inlet and outlet condition in order to make a fair comparison between fluids having different critical point [30].

A sensitivity analysis has been performed on the maximum cycle temperature, i.e., the compressor outlet temperature $T_{comp,out}$ (point 1), in order to understand its impact on system performance. Its value has been varied in a range between 160 °C (few Celsius degrees above the HP condensation temperature) and 180 °C, that is nowadays the maximum temperature reached by high temperature heat pumps [31].

The compressor inlet temperature (point 4_r) is then determined from the knowledge of compressor outlet temperature, the compressor pressure ratio, and the assumed compressor isentropic efficiency ($\eta_{is,comp}$): as the compressor inlet temperature (4_r) generally results higher than the saturation temperature at evaporation pressure (1_v), the use of a recuperator is required for preheating vapors by cooling down the saturated liquid (2) before the throttling valve inlet (2_r).

The duty and size of the recuperator is a function of the fluid complexity and the desired compressor outlet temperature, and it must be noted that for very complex working fluids characterized by a strongly overhanging saturation dome, the recuperator is always required to avoid two-phase flow compression.

Table 1 Assumptions for the computation of the HP thermodynamic cycle

Parameter	Value
Reactor thermal power input, kW	1000
Charging reaction temperature $T_{react,CH}$, °C	150
Waste heat source inlet temperature $T_{WH,in}$, °C	100
Waste heat source outlet temperature $T_{WH,out}$, °C	80
Evaporator equivalent pressure drop $\Delta T_{2\,ph,EVA}$, °C	0.5
Condenser equivalent pressure drop $\Delta T_{2\,ph,COND}$, °C	1
Desuperheater relative pressure drop	0.5%
Recuperator relative pressure drop (hot/cold)	2%
Compressor isentropic efficiency $\eta_{is,comp}$	80%
Compressor mechanical efficiency	97%
Motor electrical efficiency	97%
Evaporator pinch point temperature difference, °C	2
Condenser pinch point temperature difference, °C	2

Downloaded from http://asmedigitalcollection.asme.org/gasturbinespower/article-pdf/146/10/101013/7343132/gtp_146_10_101013.pdf by Politecnico Di Milano user on 09 July 2024

Throttling valve outlet condition (3) is eventually determined by assuming an isenthalpic process from recuperator hot side outlet condition (3_r).

Pressure drops for both sides of the recuperator are considered equal to 2% with respect to the inlet pressure. Table 1 reports all the assumed parameter values for the calculation of HP cycle. The working fluid mass flowrate is calculated from an energy balance at the reactor being the thermal duty set to 1 MW.

Once all the thermodynamic streams are determined, the sizing of the heat exchangers is carried out by adopting a discretized (50 sections) and iterative approach which depends on the type of heat exchanger and architecture of system (coupled cycles/decoupled cycles):

- **High pressure heat exchanger**: fluid condensation and de-superheating are carried out in the coiled tubes of the stirred reactor acting as a once-trough heat exchanger. Tube diameter and tube thickness are fixed, and inlet fluid velocity is determined to match the assumed overall pressure drop. Number of tubes is then calculated, and the tube length and overall heat transfer surface are eventually retrieved knowing the local overall heat transfer coefficient obtained by the combination of internal heat transfer coefficient (working fluid side) and the external one (stirred reactor side), plus the metal conductive resistance.
- Gnielinski correlation [32] is adopted for vapor working fluid de-superheating, Cavallini correlation [33] is implemented for condensation (requiring an additional internal iterative procedure for the determination of the tube wall temperature), while the external heat transfer coefficient is assumed constant and equal to a conservative value of 2000 W/m^{2}K, as suggested from Ref. [34]. Pressure drops are calculated only considering the frictional contribution for vapor and two-phase flow regime.
- **Low pressure heat exchanger**: in case of coupled cycles architecture, the fluid evaporation is carried out in a shell-and-tube once-through heat exchanger and, also in this case, the number of tubes is found iteratively to match the assumed pressure drops.
- Liu and Winterton correlation [35] is adopted for the heat transfer coefficient in flow boiling conditions (requiring an additional internal iterative procedure for the determination of the heat flux) while the external heat transfer coefficient (hot water from a renewable source or waste heat) is calculated with Zukauskas correlation [36] by assuming a fixed longitudinal and transversal tube pitch, a fixed tube arrangement and a fixed baffle spacing with respect to shell diameter. Working fluid pressure drops in evaporation are calculated only considering the frictional contribution.
- A co-current heat exchanger is adopted in order to increase the evaporation temperature and improve the COP as discussed in Sec. 4.2. In the case of decoupled cycles, a conventional kettle reboiler is adopted. In this case, pressure drops are set to zero and the calculation is not iterative. Cooper correlation [37] is adopted for evaporation side while, for hot water, Gnielinski correlation is adopted with the same tube diameter and a water velocity equal to 2 m/s to avoid damage wear and tear of the HX pipes.
- **Recuperator**: a finned tube battery heat exchanger is implemented considering liquid fluid flowing in tubes and vapor flowing on the external finned surface in cross flow. The number of tubes and tube pitch calculation relies on an iterative procedure to match the pressure drops on liquid and vapor side, respectively. Gnielinski and Zukauskas correlations are used for the computation of liquid and vapor heat transfer coefficients, respectively. A fixed $A_{ext,tot}/A_{int}$ ratio equal to around 11 is adopted, as suggested in Ref. [38].

Fouling resistance has been neglected for the design of all the heat exchangers while all the other assumptions related to heat exchanger sizing are reported in Table 2.

Table 2 Assumption for the preliminary sizing of the heat exchangers for the coupled cycles systems

Heat exchangers tubes	
Tube internal diameter, mm	25
Tube thickness, mm	2
Tube internal roughness, mm	10^{-3}
Material	SS316
HP evaporator (low pressure HX)	
Tube arrangement	Staggered
Ratio of longitudinal tube pitch to ext. diameter	1.25
Ratio of transverse tube pitch to ext. diameter	1.25
Relative baffle spacing to shell diameter	0.2
Recuperator	
Ratio of longitudinal tube pitch to ext. diameter	1.75
Ratio of transverse tube pitch to ext. diameter	1.75
Finned external to internal surface ratio	11

3.2 Discharging Mode: Power Unit Cycle. Power unit cycle is assumed as a saturated organic Rankine cycle implementing the recuperator if already required by the heat pump cycle. As heat is released at constant temperature from the reactor, the adoption of fluid superheating is not advantageous in this specific case. Superheating the fluid would simply result in a reduction of evaporation pressure and a penalization of cycle performance while, on the other hand, the use of complex fluids guarantees the avoidance of two-phase flow expansion even starting from saturated vapor conditions. The main assumptions regard the reactor discharging temperature ($T_{react,DCH}$), district heating supply temperature ($T_{supply,DH}$), which have been set respectively equal to 130 °C, as suggested by experimental activities at TUW labs, and 60 °C, as representative of fourth DH generation [39]. In the case of decoupled cycles architecture, the calculation procedure is very similar to the charging one, and it is reported in Fig. 3 on the right. The assumed pinch points and pressure drops on evaporator, condenser, and recuperator are reported in Table 3. Sizing of heat exchangers follows the same procedure already explained for the charging cycle with the only difference related to the condenser: in this case, a shell-and-tube architecture is implemented with district heating water flowing in the tubes and vapor condensing on the shell side. Nusselt modeling [40] is adopted for film condensing while for cold water, the Gnielinski correlation is adopted considering the same tube internal diameter and a water velocity of 2 m/s.

Differently, in the case of coupled cycle architecture, the determination of evaporation temperature, condensation

Table 3 Assumptions for the computation of the PU thermodynamic cycle

Parameter	Value
Reactor thermal power output, kW	1000
Discharging reaction temperature $T_{react,DIS}$, °C	130
DH water delivery temperature $T_{DH,del}$, °C	60
DH water return temperature $T_{DH,ret}$, °C	35
Turbine isentropic efficiency η_{turb}	90%
Pump hydraulic efficiency η_{pump}	80%
Turbine/pump mechanical efficiencies	97%
Motor/generator electrical efficiencies	97%
Only for decoupled cycles	
Evaporator pinch point temperature difference, °C	2
Condenser pinch point temperature difference, °C	2
Recuperator pinch point temperature difference, °C	3
Evaporator equivalent pressure drop $\Delta T_{2\,ph,EVA}$, °C	1
Condenser equivalent pressure drop $\Delta T_{2\,ph,COND}$, °C	0.5
Economizer relative pressure drop	2%
Desuperheater relative pressure drop	0.5%
Recuperator relative pressure drop (hot/cold)	2%

Downloaded from http://asmedigitalcollection.asme.org/gasturbinespower/article-pdf/146/10/101013/7343132/gtp_146_10_101013.pdf by Politecnico Di Milano user on 09 July 2024

temperature, recuperator pinch point temperature difference, and pressure drops in each heat exchanger is based on the off-design operation of the components already sized in charging mode. Knowing the number of tubes, their length, and the heat transfer area, the fluids' outlet thermodynamic conditions are determined iteratively adopting the same correlations for heat transfer and pressure drops already implemented in charging mode. Also, for the PU, the low pressure heat exchanger (condenser) is operated in cocurrent flow arrangement in order to have the largest local temperature difference in the desuperheating process, which is characterized by the lowest working fluid heat transfer coefficient. This approach allows to significantly increase the system RTE as discussed in Sec. 4.2.

Reactor power in discharging mode is set equal to the reactor power in charging mode, thus considering the same charging and discharging time. Of course, this assumption is not mandatory, and the final design of the system must be tailored to the specific investigated application. For example, it is reasonable that residential applications would require a larger heat pump size, working fewer hours a year during summer, and exploiting the availability of electrical renewables only in off-peak periods, and a smaller size power unit working steadily during winter period for a longer time. In this latter case, power unit performance would be higher than that provided in this paper since all the heat exchangers would be oversized in discharge mode. Similarly, no heat integration is considered in discharging mode in order to consider the most conservative case: if renewable or waste heat is available also during winter period, it is then possible to reduce the PU condensation temperature and improve the system performance.

3.3 Figures of Merit Calculation. The H2020 RESTORE project has the main goal to provide an effective solution for unlocking the possibility to dispatch a large amount of thermal energy on seasonal scale. This result could be obtained independently on the working fluid selected, the compressor outlet temperature, or the cycle architecture adopted. On the contrary, dispatchability and storage of electricity are secondary features whose performance actually varies consistently depending on the system design. For this reason, the overall RTE of the system is selected as the main figure of merit for the comparison of different working fluids. Electrical RTE is defined as the ratio between the net power released by the power unit cycle and the electrical power absorbed by the heat pump cycle, according to the assumption of same number of charging and discharging hours. In this preliminary analysis, the additional auxiliary consumption related to the water circulation and stirring of the reactor is neglected for both the charging and discharging cycle. It must be noted that this definition is equivalent to the product between the heat pump coefficient of performance (COP_{HP}) and the power unit electrical efficiency (η_{PU}) as reported in the following equation:

$$RTE = \frac{\dot{W}_{turb,el,PU} - \dot{W}_{pump,el,PU}}{\dot{W}_{comp,el,HP}} = COP_{HP} \cdot \eta_{PU} \quad (2)$$

In addition to the system RTE, the ratio between RTE and overall heat exchanger surface (RTE/A_{tot}) is adopted as parameter representative of the techno-economic tradeoff between system performance and investment cost which, considering the low power/heat ratio of this application (high heat pump COP and rather low power unit efficiency), is likely dominated by heat exchangers equipment.

Finally, volume ratio and maximum volumetric flowrate for both compressor and turbine are monitored as important parameters for the comparison of turbomachinery size and cost for different working fluids. Maximum volumetric flow rates (compressor intake and turbine discharge) directly affect turbomachinery frontal area while the number of stages is generally determined by the need of overall volume ratio repartition, since blade loading is generally limited for high molecular mass working fluids, as in this case.

Since the performance of the different components (and, in particular, the turbine and the compressor) is not affected by the equipment size, COP_{HP}, η_{PU}, RTE, $RTE/A_{tot,}$ and turbomachinery volume ratio (V_r) are only function of the working fluid (and its operating conditions) while mass and volumetric flow rates can be scaled up and scaled down linearly for different system size.

4 Results and Discussion

Results are obtained by investigating the performance of the coupled system with 16 different working fluids (preselected from a wider pool of over 30 fluids) while the performance of the decoupled system is obtained by combining the results for the heat pump and power unit cycles obtained for all the working fluids, for a total amount of 256 cases. Table 4 lists the investigated working fluids and their critical temperature, global warming potential (GWP) and Health, fire and instability hazard (HFI) indexes as defined by national fire protection agency (NFPA) [41]. Most of the selected fluids are hydrocarbons, a promising class of fluids for this application, spanning in a large range of critical temperatures and having low GWP (generally below 5 likely also for fluids whose index is not reported due to the lack of available data), although they are flammable and, in some cases, slightly toxic (Benzene, Xylenes, Dimethyl carbonate). Only few halogenated fluids with sufficiently high critical temperature for this specific application have been included while several others (i.e., perfluoro-propane, R227ea, perfluoro-cycle-propane, perfluoro butane) have been excluded since they show extremely high GWP (between 3000 and 10,000), and their use is discouraged by their progressive phase out. Siloxanes are not included in the list as well, due to their high critical temperatures, which makes them not the preferable choice for such low temperature applications. Two preliminary discussions on the effect of compressor outlet temperature and heat exchangers arrangement are provided only for cyclopentane, as it has been identified as one of the most promising working fluids for this specific case study.

4.1 Effect of Compressor Outlet Temperature. Increasing the compressor outlet temperature has a positive effect on the system performance. For a given fluid, with a fixed minimum temperature of the renewable or waste heat source and a fixed reactor charging temperature, a higher compressor outlet temperature implies a higher compressor inlet temperature: compressor-specific work increases but the fluid mass flowrate reduces because of the larger working fluid enthalpy change between reactor inlet (1) and outlet (2). For a fixed reactor duty, the compressor power decreases leading

Table 4 Investigated working fluids and their critical temperature, global warming potential (GWP) and HFI indexes as defined by NFPA

				NFPA		
#	Fluid	T_{crit}, °C	GWP	H	F	I
1	Trans-2-butene	155.46	N.A.	1	4	0
2	Cis-2-butene	162.60	N.A.	1	4	0
3	Novec649	168.66	1	3	1	0
4	R365mfc	186.85	794	0	4	1
5	Isopentane	187.20	5	1	4	0
6	Isohexane	224.55	<1	2	3	0
7	Cyclopentane	238.57	5	1	3	0
8	Cyclohexane	280.45	2	1	3	0
9	Dimethyl carbonate	283.85	<1	3	3	0
10	Benzene	288.87	N.A.	2	3	0
11	Octane	295.59	4–6	1	3	0
12	Para-xylene	343.02	N.A.	2	3	0
13	Metaxylene	343.74	N.A.	2	3	0
14	Decane	344.55	4–6	1	2	0
15	Orto-xylene	357.11	N.A.	2	3	0
16	Propyl-cyclohexane	357.65	4-6	1	3	0

Downloaded from http://asmedigitalcollection.asme.org/gasturbinespower/article-pdf/146/10/101013/7343132/gtp_146_10_101013.pdf by Politecnico Di Milano user on 09 July 2024

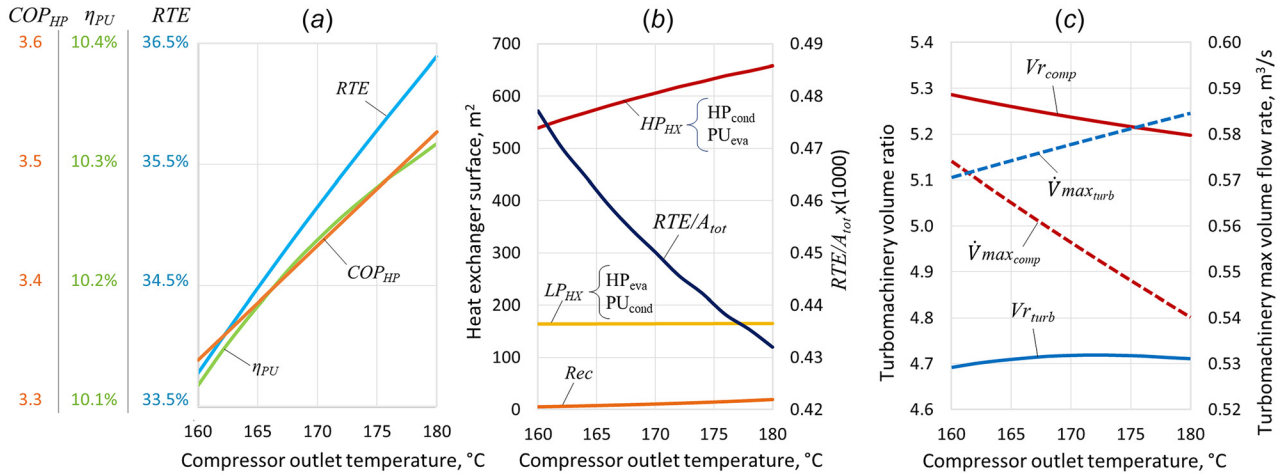

Fig. 5 Trend of relevant parameters for coupled systems working with cyclopentane versus compressor outlet temperature: (*a*) HP COP, PU efficiency and system RTE, (*b*) heat exchangers surface and overall RTE/A_{tot}, and (*c*) volume ratio and maximum volumetric flowrate for compressor and turbine

to an increase of COP_{HP}. In the case of coupled systems, there is an additional benefit related to the increase of the recuperator heat transfer surface required to preheat working fluid vapors before compression, as it also allows to increase η_{PU} in discharging mode. Figure 5(*a*) depicts the sensitivity analysis on compressor outlet temperature for cyclopentane in a coupled cycles architecture. It is possible to highlight that the RTE increases from 33.8% to 36.4% (+7.7%) when passing from 160 °C to the maximum allowable compressor outlet temperature, equal to 180 °C. This beneficial effect is mainly due to an increase of COP_{HP}, which passes from 3.34 to 3.53 (+5.7% on relative base), and only marginally from an improvement of η_{PU}, which increases from 10.1% to 10.3% (+2% on relative base). Figure 5(*b*) depicts the trend of heat exchanger surfaces against compressor outlet temperature: as the compressor outlet temperature increases, recuperator size clearly increases because of the larger thermal duty and the lower pinch point temperature difference. However, for cyclopentane, the recuperator size is marginal with respect to the other heat exchangers. Low pressure heat exchanger surface just marginally increases due to slightly larger thermal duty of the component due to the higher COP_{HP}. Finally, the heat transfer surface of the coiled stirred reactor (high pressure heat exchanger), which represents the largest component of the system, shows an increasing trend with compressor outlet temperature, as the larger temperature difference in the desuperheating process does not compensate for the lower local heat transfer coefficient of this section compared to the condensing one.

As a result, the total heat exchangers surface increases by 19% at maximum compressor outlet temperature, causing a reduction of the RTE/A_{tot} parameter, which accounts for the tradeoff between efficiency gains and increase in heat transfer equipment size. Figure 5(*c*) reports the effect of compressor outlet temperature on turbomachinery parameters, namely, volume ratio and volumetric flowrate. Compressor volume ratio (V_r) slightly decreases since the compression process is farther from the saturation dome and characterized by lower real gas effects, while volumetric flowrate at compressor intake reduces since the reduction of mass flowrate is not balanced by the decrease of inlet fluid density caused by the temperature increase. Regarding the expander, the effect on volume ratio is nearly negligible since the compressor outlet temperature only slightly affects the evaporation temperature in discharging mode, while the turbine outlet volumetric flowrate increases because of the slightly lower condensing pressure.

In conclusion, the increase of compressor outlet temperature for cyclopentane benefits the system performances by 7.7%, but causes an increase of 19% of heat exchangers surfaces and a reduction of 6% of turbomachinery dimension and thus seems to be profitable only in cases with very high remuneration of electricity during discharge operation.

These considerations in relative terms are generally valid for most of the investigated fluids but those characterized by very low critical temperatures, as further discussed in Sec. 4.3.

Another observation is related to the possibility to operate fully reversible cycles, where also the compressor/expander is actually the same component operated reversibly: volume ratio in expansion is slightly lower than in compression (around -10%), thus implying the feasibility of operating the same volumetric machine in both operative modes.

4.2 Effect of Low-Pressure Heat Exchanger Flow Arrangement. A sensitivity analysis is carried out varying the flow arrangement of the low-pressure heat exchanger, namely, adopting the four combinations given by cocurrent and countercurrent flow arrangement in charging mode (HP evaporator) and discharging mode (PU condenser).

Table 5 summarizes the results of this analysis applied to the coupled cycle architecture working with cyclopentane. Having a countercurrent arrangement in the HP charging cycle (design mode) implies a larger heat exchanger heat transfer area, even if this difference is rather limited (around 7%), and a slightly lower COP_{HP}. On the contrary, flow arrangement in discharging PU mode has a much higher impact on system performance: a countercurrent disposition implies a much higher condensation temperature for the power unit (around +3 °C), a larger pinch point (around +5.5 °C) as a consequence of the larger heat transfer surface required for the fluid desuperheating. On the contrary, adopting a cocurrent disposition the efficiency of the power unit is increased (+0.5

Table 5 Results of the sensitivity analysis on the low-pressure heat exchanger flow arrangement

Case	A	B	C	D
HP_{eva}	Counter-c	Co-c	Counter-c	Co-c
PU_{cond}	Counter-c	Counter-c	Co-c	Co-c
LP_{HX}, m^2	176.4	164.8	176.4	164.8
PU T_{cond}, °C	64.7	65.6	61.6	62.0
PU $\Delta T_{pp,cond}$, °C	6.4	7.4	1.6	2
COP_{HP}	3.41	3.43	3.41	3.43
η_{PU}	9.86%	9.71%	10.30%	10.24%
RTE	33.6%	33.3%	35.1%	35.15%

Downloaded from http://asmedigitalcollection.asme.org/gasturbinespower/article-pdf/146/10/101013/7343132/gtp_146_10_101013.pdf by Politecnico Di Milano user on 09 July 2024

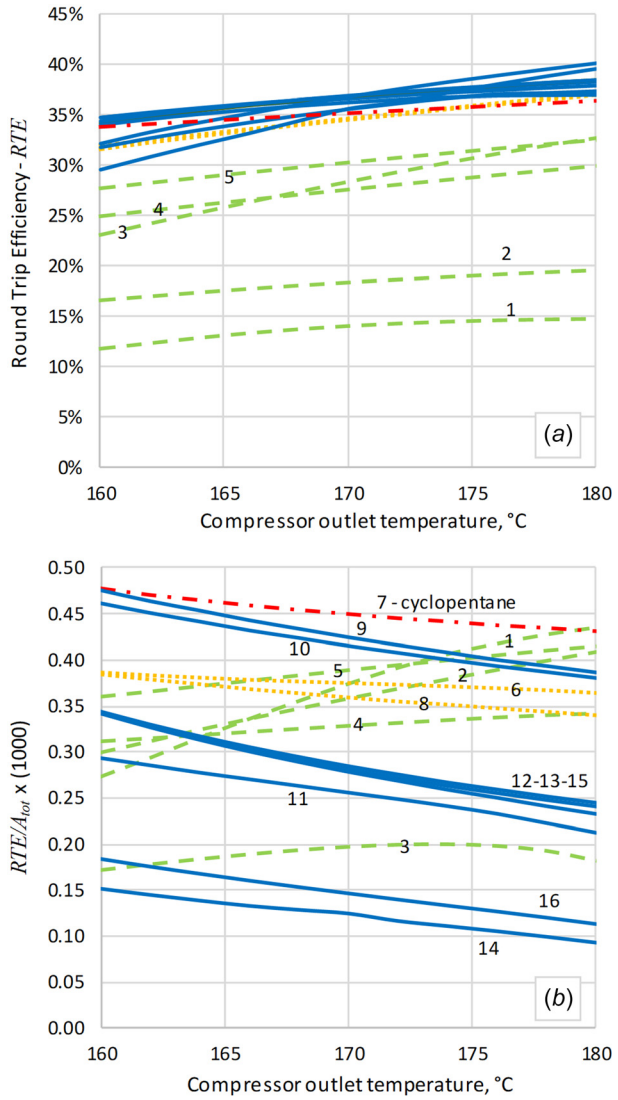

Fig. 6 Trend of relevant parameters for coupled systems versus compressor outlet temperature: (*a*) system RTE and (*b*) overall RTE/A_{tot}

points of efficiency) thanks to a lower condensation temperature, as well as the overall RTE of the system (+2 points of efficiency and +6% on relative base).

4.3 Working Fluid Selection for Coupled Cycle Architecture. Figure 6 depicts the trend of RTE and RTE/A_{tot} as function of the compressor outlet temperature for the 16 fluid candidates in coupled system configuration. It is possible to highlight that by increasing the compressor outlet temperature the RTE (Fig. 6(*a*)) increases for all the investigated fluids and that most of them show a quite similar RTE: in particular, adopting low critical temperature fluids does not appear as a promising solution mainly due to the low achievable COP_{HP}.

On the contrary, the discussion related to the RTE/A_{tot} (Fig. 6(*b*)) parameter is less trivial since the trend of the total heat transfer area is different depending on the fluid critical temperature. By increasing the compressor outlet temperature for low critical temperature fluids (dashed lines in figure) the desuperheating section is characterized by relatively high local heat transfer coefficients (thanks to the higher fluid density) that, combined with the higher local temperature difference, entails a reduction of high-pressure heat exchangers surfaces (i.e., coiled heat exchanger in the stirred reactor) and thus an increase of the RTE/A_{tot} parameter. For fluids with intermediate critical temperatures (yellow dotted lines in figure), as cyclopentane (red dash-dotted line), the increase of heat transfer area implies a slight reduction of the RTE/A_{tot} parameter. Finally, higher critical temperature fluids (blue solid lines) show very low condensing pressure in HP mode involving very low heat transfer coefficients for organic vapors and a soaring of the heat transfer area required for fluid desuperheating, being this section always designed with a fixed pressure drop. Thus, their RTE/A_{tot} parameter is further penalized. Cyclopentane (red line) stands out as a promising fluid from both RTE and RTE/A_{tot} perspective in the whole range of compressor outlet temperatures.

A deeper analysis is provided focusing on an intermediate compressor outlet temperature, equal to 170 °C, and reporting the figures of merit as function of fluid critical temperature. Figure 7(*a*) depicts the trend of RTE, COP_{HP}, and η_{PU}: it is possible to highlight that, with the exception of the butane isomers, all the other fluids show nearly the same PU efficiency while they strongly differ in COP_{HP}, which varies by 70% within the fluid critical temperature range investigated in this work.

As result, RTE initially strongly benefits by adopting working fluids with a higher critical temperature and then flatten above a critical temperature of around 250 °C. Figure 7(*b*) depicts the total HXs area and COP_{HP} parameter against fluid critical temperature.

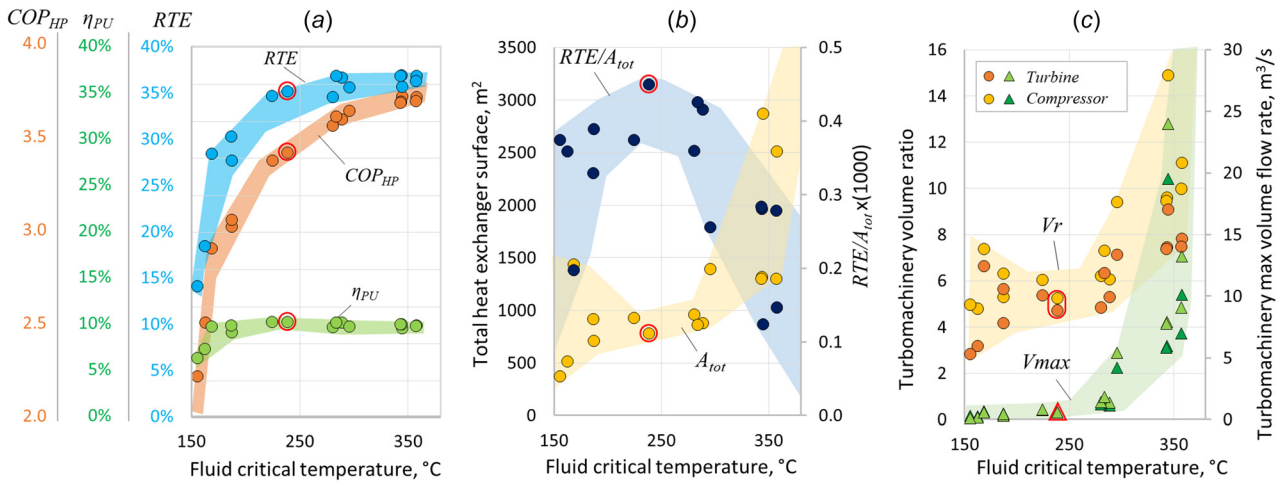

Fig. 7 Trend of the relevant parameters for coupled systems with all fluids versus critical temperature: (*a*) HP COP, PU efficiency and system RTE, (*b*) heat exchanger surface and overall RTE/A_{tot}, and (*c*) volume ratio and maximum volumetric flowrate for compressor and turbine. The additional envelopes on the markers identify solutions employing cyclopentane as working fluid.

Downloaded from http://asmedigitalcollection.asme.org/gasturbinespower/article-pdf/146/10/101013/7343132/gtp_146_10_101013.pdf by Politecnico Di Milano user on 09 July 2024

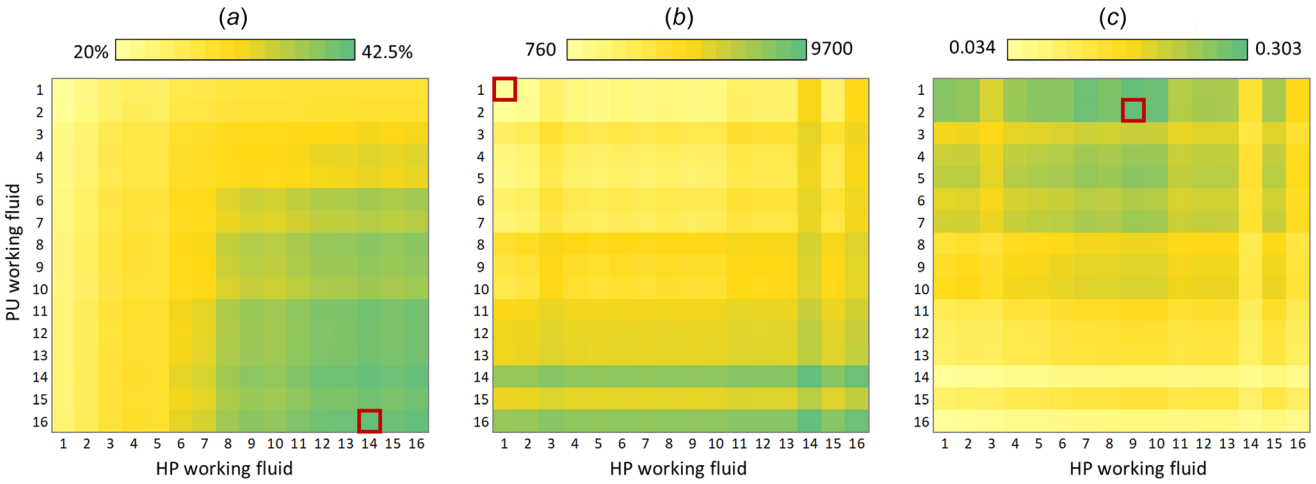

Fig. 8 Contour maps of the most relevant parameters for decoupled systems for all the working fluids combinations: (*a*) system RTE, (*b*) total heat exchangers surface, and (*c*) overall RTE/A_{tot}

Total heat transfer area increases with the fluid critical temperature due to the exponential decrease of cycle pressure levels and thus, being the heat exchanger designed with the same relative pressure drops, a strong penalization in the heat transfer coefficients: in particular, the recuperator gradually becomes a relevant share of the overall heat transfer area. RTE/A_{tot} parameter accounts for these effects and shows a trend with a maximum. Finally, Fig. 7(*c*) depicts the trend of volume ratio and volumetric flow rates. Volume ratio is relatively constant and lower than 10 for fluids with critical temperature below 300 °C while rapidly increases for higher values, implying the use of multistage turbine and compressors. Similarly, volume flow rates exponentially increase with fluid critical temperature, leading to larger and more expensive machines.

Those results lead to the conclusion that the choice of the working fluid shall also include techno-economic considerations since the adoption of a fluid with a too low critical temperature may penalize the system due to the lower RTE, while the adoption of a fluid with an excessive critical temperature would involve an increase of heat exchanger (i.e., higher total heat transfer area) and turbomachinery cost (i.e., higher frontal area and number of stages). Among the investigated fluids, cyclopentane looks particularly promising, being able to reach a high RTE (>35%), to maximize the RTE/A_{tot}, to limit the volume ratio to reasonable values for single stage (or, at maximum, two-stages) radial machines, and it does not show excessive volume flow rates.

4.4 Working Fluid Selection for Decoupled Cycle Architecture. The adoption of two different separate cycles for the charging and discharging operation may be of interest with the goal of maximize system performance, thanks to the selection of the most suitable working fluids for the HP and the PU cycle, and the design of dedicated heat exchangers for both systems relying on more conventional component types. Figure 8 reports colored maps of RTE, total heat transfer area, and overall RTE/A_{tot} parameter obtained for the 256 working fluid combinations, considering a compressor outlet temperature of 170 °C. RTE (Fig. 8(*a*)) increases remarkably by adopting high critical temperature fluids for the HP cycle, while it is less affected by working fluid choice on the PU cycle, where the maximum performance achievable are rather stable against fluid choice, as already highlighted in Fig. 7(*a*). From a thermodynamic performance perspective (RTE maximization), there is no need to select two very different fluids for the HP and PU cycles, thus leading to results similar to coupled cycles systems: optimal combination is Decane and Propyl-cyclohexane for HP and PU cycles, respectively, reaching a RTE equal to 42.5%. On the contrary, from a techno-economic perspective, it would be interesting to adopt a high critical temperature fluid for the HP cycle and a lower critical temperature fluid for the PU cycle, to attain a smaller heat transfer area of the heat exchangers (Fig. 8(*b*)), a lower turbine size (lower volume ratio and volumetric flowrate), maintaining a competitive PU efficiency. As a result, the decoupled cycles system with the maximum RTE/A_{tot} (Fig. 8(*c*)) adopts dimethyl carbonate (DMC) for the HP cycle and Cis-2-butene for the PU cycle, reaching a RTE/A_{tot} value equal to 0.303, which is more than 30% lower than the best coupled cycle architecture with cyclopentane discussed in Sec. 4.3. Other fluid combinations, especially those adopting high critical temperature fluids for the PU, are strongly penalized and, from a techno-economic perspective, can only reach RTE/A_{tot} values one order of magnitude lower. Those considerations demonstrate that the use of two decoupled cycles is not likely to be a promising solution for this specific case. However, the analysis also suggests that different conclusions can be obtained in cases where the charging and discharging cycles are different in size and annual operating hours, namely, a large size HP and a small size PU (or vice versa): in this case, the different working fluid mass flow rates and power input/output may lead to the adoption of different working fluids to obtain a more feasible turbomachinery and heat exchangers design.

4.5 Comparison Among Selected Designs. Table 6 reports the main results for the maximum RTE and the maximum RTE/A_{tot} systems in both coupled and decoupled architectures, for a compressor outlet temperature of 170 °C. In coupled cycles architecture, the maximization of RTE using metaxylene as working fluid allows to reach a RTE only 2% higher than a system with cyclopentane, but it requires nearly two times the heat transfer area (strong reduction of RTE/A_{tot}), around two times the volume ratio on

Table 6 Main results for the selected designs

Coupled	max RTE	max RTE/A_{tot}
Fluid	Metaxylene	Cyclopentane
RTE	37%	35%
RTE/A_{tot}	0.28	0.45
Vr comp-turb	9.6–7.5	5.2–4.7
$\dot{V}_{max}$ comp-turb, m^3/s	5.9–7.9	0.55–0.58
Decoupled	**max RTE**	**max RTE/A_{tot}**
Fluid HP	Decane	Dimethyl carbonate
Fluid PU	Propyl-cyclohexane	Cis-2-butene
RTE	42.4%	33%
RTE/A_{tot}	0.044	0.3
Vr comp-turb	14.9–10.3	7.3–4.3
$\dot{V}_{max}$ comp-turb, m^3/s	19.5–15.0	1.4–0.18

Downloaded from http://asmedigitalcollection.asme.org/gasturbinespower/article-pdf/146/10/101013/7343132/gtp_146_10_101013.pdf by Politecnico Di Milano user on 09 July 2024

Table 7 Capital cost breakdown for the three coupled cycles systems working with hydrocarbons with different critical temperatures

Working fluid	Cyclo-pentane	Trans-2-butene	Octane
$\dot{W}_{el,in}$, MW	2.91	4.50	2.73
$\dot{W}_{el,out}$, MW	1.02	0.63	0.97
HP HX, k€	3152	1750	4868
LP HX, k€	888	381	1545
REC, k€	111	75	770
Compressor, k€	1221	1493	2224
Turbine, k€	427	215	685
Pump, k€	25	55	13
Motor-generator, k€	17	18	17
BOP, k€	1168	798	2024
Total cost, k€	7009	4785	12147
Specific cost, €/kW$_{el}$	6846	7565	12476
Specific cost with economies of scale, €/kW$_{el}$	3423	3782	6237

turbomachinery and one order of magnitude higher volumetric flow rates.

Considering that the system is fully cogenerative and electricity is not the only output with an economic value, there is not real need of pushing toward RTE maximization if this implies a dramatic increase of capital cost and thus the system optimal design shall be oriented toward maximum RTE/A_{tot}.

Similar considerations can be listed also for decoupled cycles architecture: maximization of RTE by selecting the most efficient working fluid can lead to a consistent increase of performance up to over 42%, but this result is obtained thanks to the adoption of heat exchangers with very large surfaces that in turn lead to small RTE/A_{tot} and likely to a noncompetitive system. Differently, aiming at RTE/A_{tot} maximization leads to the selection of two very different working fluids for the two systems: a midhigh critical temperature fluid for the HP cycle to maximize COP and a low critical temperature fluid for the PU cycle in order to limit the heat transfer area required by discharging cycle. In this latter case, the dimension of the turbine can also benefit from the reduced volume ratio and volumetric flow rates.

5 Preliminary Economic Analysis

A preliminary economic analysis of the profitability of the proposed technology is presented in order to highlight the effects on the PBT of different assumptions related to the electricity and the heat prices. Three coupled power systems are considered working with: (i) cyclopentane, being the fluid with the most promising critical temperature as highlighted in the previous analysis; (ii) trans-2-butene, as representative of fluids having a lower critical temperature and thus penalized in both RTE and RTE/A_{tot} ratio, and (iii) octane, as representative of fluids having a critical temperature higher than the optimal one and thus penalized in both RTE/A_{tot} ratio and turbomachinery sizing but able to achieve a higher RTE. The capital cost of the three power plants has been calculated adopting the cost functions correlations for ORC components proposed in Ref. [42], which were obtained by fitting different Refs. [43–45] and then actualized accounting for inflation factor to 2022. Shell-and-tube HXs cost correlation depends on both heat transfer area and pressure, and it is adopted for both the high-pressure and the low-pressure heat exchangers. On the contrary, finned tube recuperator cost depends only on heat transfer area. The turbomachinery cost correlation depends on the shaft power, the machine overall size parameter ($SP = V_{out}^{0.5}/\Delta h_{is}^{0.25}$), and the number of stages, calculated by imposing a maximum stage volume ratio equal to 1.5 and 4 for the HP compressor and PU expander, respectively. This design criterion is selected as organic fluids usually have high molecular mass and thus blade loading is generally not the most critical limitation for stage number definition. Generator and motor cost functions depend on the electrical power while, for the pump, both power and outlet pressure are considered.

A contribution equal to 20% of the overall installation cost is accounted for the balance of plant (BOP), including piping, instrumentation, and control costs. The cost breakdown for a 10 MW reactor system is reported in Table 7, where it is possible to highlight that cyclopentane in coupled configuration is the system with the lowest specific cost referred to the electrical power output. Trans-2-butene is characterized by a low system cost but is penalized by the low RTE (14%), while octane in coupled configuration, despite the larger RTE (36%), is penalized because of the high capital cost, mainly related to the increase of heat transfer surface and turbine size.

Cyclopentane specific cost (6800 €/kW$_{el}$) is slightly higher than the maximum value (5500 €^{2022}/kW) for commercial ORC having the same electrical power output, as reported in Ref. [46]. This is due to (i) the presence of the compressor, whose higher number of stages strongly affects the cost; (ii) the very high specific heat transfer area (m^2/MW) of the high pressure heat exchanger due to the assumption of a very narrow pinch point temperature difference (ΔT_{pp}) equal to 2 °C; and (iii) the fact that generally, a capital cost estimation resulting from the sum of equipment costs implies an overestimation of the overall cost as it neglects component standardization and scale economies in production. Considering that commercial high temperature heat pumps and commercial ORC can have specific cost around 1000–2000 €^{2022}/kW, it is reasonable to expect an overall power system cost reduction of at least 50% at the end of the technology commercialization process. All these considerations and cost differences are, however, dampened by the additional cost related to the energy storage itself, which has been estimated by considering 4 months of full operation in discharge, a reaction energy density of solids equal to 2 GJ/m^3, a solid density equal to 2400 kg/m^3 and a solid bulk cost of 0.1 €/kg, representative for $MgSO_4$ or $CaCl_2$. Adopting these assumptions, the cost of the storage (including a 20% BOP for solids containment and handling) is around 15 M€, corresponding to around 2.5 times the cost of the overall commercial power system for cyclopentane case.

The nondiscounted PBT is affected by both the capital cost and the revenues related to the electricity and heat selling (or the equivalent avoidance of energy purchase due to self-production). Four cases are considered combining two values for the electricity (40 and 300 €/MWh [47]) and heat price (80 and 170 €//MWh [48]), the first equal to the European Union average value up to 2021, the second as representative of 2022, characterized by a fossil fuels price sudden increase due to the Russian invasion of Ukraine.

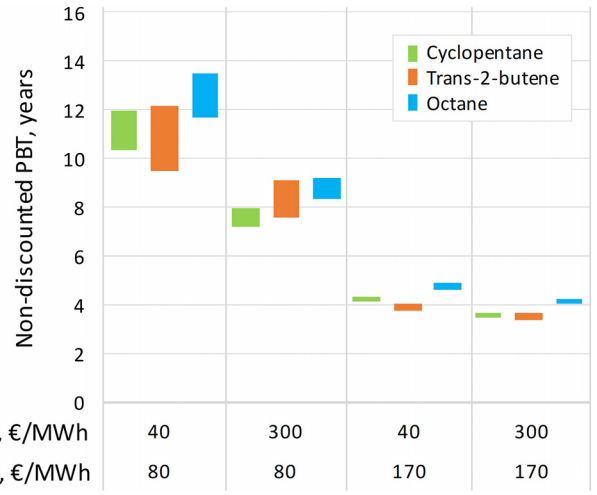

Fig. 9 Nondiscounted PBT for the three selected working fluids. For each bar the lowest value corresponds to free electricity during charge phase while the upper value considers a charging cost of 30 €/MWh.

Downloaded from http://asmedigitalcollection.asme.org/gasturbinespower/article-pdf/146/10/101013/7343132/gtp_146_10_101013.pdf by Politecnico Di Milano user on 09 July 2024

Additionally, two cases are investigated considering both free electricity in charging, in accordance with the use of very cheap off-peak electricity, or at low cost (30 €/MWh). Waste heat exploitation during charging is always considered free of charge while incentives or carbon credits are not included in the analysis. Figure 9 depicts the nondiscounted BPT for the selected fluids and for the eight different energy price cases. It is interesting to note that octane is not the most promising fluid regardless of the economic assumptions, while cyclopentane and trans-2-butene can compete against each other depending on the considered electricity and heat prices. In particular, trans-2-butene is more interesting for cases with lower electricity price according to the lower RTE, while cyclopentane is suggested when the ratio between the electricity price and heat price increases. Effect of charging electricity cost (span of the colored bars for each case) is more marked on the trans-2-butene due to the higher electrical consumption in HP mode. Final values of PBT in case of higher price of both electricity and heat (i.e., highest revenues) are below 4 years, but can be as high as 12 years in cases where energy is cheap for long periods. All these considerations highlight the high variability of the results that can be obtained by assuming different electricity and heat prices, suggesting that the proposed methodology is a useful tool for preselecting adequate working fluids for PTES technology, but the final choice on the cycle design must be necessarily tailored to the specific case scenario with a precise assessment of the expected trend of electricity and heat prices.

6 Conclusions

The results obtained in this paper allow to highlight the following conclusions:

- From a purely thermodynamic perspective, mid-temperature PTES systems based on organic fluids are a promising solution thanks to the better matching between the isothermal thermochemical reactor and the working fluid phase transition, which allows to minimize the reduction of the maximum temperature when passing from charging to discharging mode.
- These systems are capable to achieve maximum RTEs in the range between 35% and 40%, which are comparable with those attainable with H_2 storage from electrolysis plus power production in gas turbines or fuel cells, making the proposed solution a possible asset in future energy markets requiring seasonal electricity storage.
- The use of coupled cycles, although more complex from control perspective, allows to significantly reduce the capital cost of the system, still guaranteeing good thermodynamic performances (RTE $>$ 35%). In this case, cyclopentane appears to be one of the most recommended working fluids from a techno-economic point of view as it reaches a high RTE (35%) and the maximum RTE/A_{tot} index (0.45). It also presents small volumetric flow rates and limited compressor and turbine volume ratios, simplifying the design of the turbomachinery. The use of hydrocarbons is interesting from an environmental point of view (GWP equal to 5 and null ozone depletion potential), while their flammability is an issue already faced in most of the ORC units installed worldwide. Alternatively, high critical temperature refrigerant fluids could be used but they are currently in phase out due to their high GWP and their cost, which is getting prohibitive.
- Decoupled cycles can be of interest in case the use of a reversible system is not possible due to the difficulties in designing and operating heat exchangers alternatively as condensers with a de-superheating section and evaporators with an economizer. In this case, it would be possible to find a combination of fluids able to achieve RTE over 30% and reasonable RTE/A_{tot}.
- The proposed methodology could be a valid method for the selection of a restricted number of working fluid candidates to be further investigated with a detailed techno-economic assessment. The preliminary analysis proposed in this work highlights that working fluids characterized by a lower RTE but also a lower capital cost (i.e., trans-2-butene in the example) can be of interest since any reduction in electrical power output results in an increase in the heat release to the thermal user, which is also economically remunerated.

Acknowledgment

The current work has been developed for the RESTORE project[2]. RESTORE project has received funding from the European Union's Horizon 2020 research and innovation programme under grant agreement No. 101036766.

This paper reflects only the authors' views and opinions; neither the European Union nor the European Commission can be considered responsible for them.

Funding Data

- European Union's Horizon 2020 research and innovation program (Grant No. 101036766).
- NEST - Network 4 Energy Sustainable Transition (D.D. 1243 02/08/2022, PE00000021) and received funding under the National Recovery and Resilience Plan (NRRP), Mission 4 Component 2 Investment 1.3, funded from the European Union – NextGenerationEU.

Data Availability Statement

The datasets generated and supporting the findings of this article are obtainable from the corresponding author upon reasonable request.

Nomenclature

ACAES = adiabatic compressed air energy storage
ATES = aquifer thermal energy storage
BOP = balance of plant
BTES = borehole thermal energy storage
COP = coefficient of performance
DH = district heating
GWP = global warming potential
HFI = health, fire, and instability
HP = heat pump
HTF = heat transfer fluid
HX = heat exchanger
LAES = liquid air energy storage
NFPA = National Fire Protection Association
ORC = organic rankine cycle
PBT = payback time
PCM = phase change material
PTES = pumper thermal energy storage
PV = photovoltaic
PU = power unit
RES = renewable energy source
RTE = round trip efficiency
TES = thermal energy storage
TUW = Technical University of Wien

References

[1] International Energy Agency, 2020, "European Union 2020: Energy Policy Review," International Energy Agency, Paris, France, accessed May 3, 2024, https://www.iea.org/reports/european-union-2020

[2] Bacquet, A., Galindo Fernández, M., Oger, A., Themessl, N., Fallahnejad, M., Kranzl, L., Popovski, E., et al., 2022, *District Heating and Cooling in the European Union – Overview of Markets and Regulatory Frameworks Under the Revised Renewable Energy Directive*, Publications Office of the European Union, European Commission. European Commission. Directorate General for Energy, Luxembourg.

[2] www.restore-dhc.eu/

Downloaded from http://asmedigitalcollection.asme.org/gasturbinespower/article-pdf/146/10/101013/7343132/gtp_146_10_101013.pdf by Politecnico Di Milano user on 09 July 2024

[3] Lyden, A., Brown, C. S., Kolo, I., Falcone, G., and Friedrich, D., 2022, "Seasonal Thermal Energy Storage in Smart Energy Systems: District-Level Applications and Modelling Approaches," Renewable Sustainable Energy Rev., **167**, p. 112760.
[4] Lemmens, B., Desmedt, J., Hoes, H., and Patyn, J., 2007, "Haalbaarheidsstudie Naar de Toepassing Vankoude-Opslag Met Recirculatie Bij Kaneka te Westerlo," *Vlaamse Instelling Voor TechnologischOnderzoek*, Mol, Belgium, pp. 1–48.
[5] Fleuchaus, P., Godschalk, B., Stober, I., and Blum, P., 2018, "Worldwide Application of Aquifer Thermal Energy Storage – A Review," Renewable Sustainable Energy Rev., **94**, pp. 861–876.
[6] Lee, K. S., 2010, "A Review on Concepts, Applications, and Models of Aquifer Thermal Energy Storage Systems," Energies, **3**(6), pp. 1320–1334.
[7] Reuss, M., 2015, "The Use of Borehole Thermal Energy Storage (BTES) Systems," Woodhead Publishing Series in Energy, Advances in Thermal Energy Storage Systems (Second Edition), Woodhead Publishing, Cambridge, UK, pp. 117–147.
[8] Dahash, A., Ochs, F., Janetti, M. B., and Streicher, W., 2019, "Advances in Seasonal Thermal Energy Storage for Solar District Heating Applications: A Critical Review on Large-Scale Hot-Water Tank and Pit Thermal Energy Storage Systems," Appl. Energy, **239**, pp. 296–315.
[9] solarthermalworld.org, 2019, "Seasonal Pit Heat Storage Cost Benchmark," accessed May 1, 2024, https://solarthermalworld.org/news/seasonal-pit-heat-storage-cost-benchmark-30-eurm3/
[10] Cheung, B., Carriveau, R., and Ting, D. S.-K., 2012, "Storing Energy Underwater," ASME Mech. Eng., **134**(12), pp. 38–41.
[11] Astolfi, M., Rizzi, D., Macchi, E., and Spadacini, C., 2022, "A Novel Energy Storage System Based on Carbon Dioxide Unique Thermodynamic Properties," ASME J. Eng. Gas Turbines Power, **144**(8), p. 081012.
[12] Brett, G., and Barnett, M., 2014, "The Application of Liquid Air Energy Storage for Large Scale Long Duration Solutions to Grid Balancing," EPJ Web Conf., **79**, p. 03002.
[13] Laughlin, R. B., 2017, "Pumped Thermal Grid Storage With Heat Exchange," J. Renewable Sustainable Energy, **9**(4), p. 044103.
[14] SwRI, 2022, "Demonstrates Small-Scale Pumped Heat Energy Storage System," SwRI, San Antonio, TX, accessed May 1, 2024, https://www.swri.org/press-release/swri-demonstrates-small-scale-pumped-heat-energy-storage-system
[15] Steinmann, W. D., 2014, "The CHEST (Compressed Heat Energy STorage) Concept for Facility Scale Thermo Mechanical Energy Storage," Energy, **69**, pp. 543–552.
[16] Hassan, A. H., Corberán, J. M., Ramirez, M., Trebilcock-Kelly, F., and Payá, J., 2022, "A High-Temperature Heat Pump for Compressed Heat Energy Storage Applications: Design, Modeling, and Performance," Energy Rep., **8**, pp. 10833–10848.
[17] RESTORE, 2021, "Renewable Energy Based Seasonal Storage Technology in Order to Raise Economic and Environmental Sustainability of DHC," accessed May 1, 2024, https://www.restore-dhc.eu/
[18] MAN, 2022, "MAN ETES – A Versatile Energy Storage Solution for All Sectors," accessed May 1, 2024, https://www.man-es.com/energy-storage/solutions/energy-storage/electro-thermal-energy-storage
[19] Held, T. J., 2021, "Low-Cost, Long-Duration Electrical Energy Storage Using a CO2-Based Electro Thermal Energy Storage (ETES) System. Echogen Power Systems,".
[20] Siemens Gamesa Renewable Energy, 2021, "ETES – Electric Thermal Energy Storage – Technology and Commercial Proposition," Siemens Gamesa Renewable Energy, Hamburg, Germany.
[21] Pintail Power, 2020, "Large-Scale, Long- Duration Energy Storage," Pintail Power, Palo Alto, CA, accessed May 1, 2024, https://www.pintailpower.com/
[22] ENEL, 2022, "Introducing TES, an Energy Storage Technology Inspired by Nature," accessed May 1, 2024, https://www.enelgreenpower.com/media/news/2022/11/storage-system-tes-santa-barbara
[23] Sarbu, I., and Dorca, A., 2019, "Review on Heat Transfer Analysis in Thermal Energy Storage Using Latent Heat Storage Systems and Phase Change Materials," Int. J. Energy Res., **43**(1), pp. 29–64.
[24] Steger, D., Regensburger, C., Eppinger, B., Will, S., Karl, J., and Schlücker, E., 2020, "Design Aspects of a Reversible Heat pump-Organic Rankine Cycle Pilot Plant for Energy Storage," Energy, **208**, p. 118216.
[25] Eppinger, B., Zigan, L., Karl, J., and Will, S., 2020, "Pumped Thermal Energy Storage With Heat pump-ORC-Systems: Comparison of Latent and Sensible Thermal Storages for Various Fluids," Appl. Energy, **280**, p. 115940.
[26] Dumont, O., and Lemort, V., 2020, "Mapping of Performance of Pumped Thermal Energy Storage (Carnot Battery) Using Waste Heat Recovery," Energy, **211**, p. 118963.
[27] Jockenhöfer, H., Steinmann, W.-D., and Bauer, D., 2018, "Detailed Numerical Investigation of a Pumped Thermal Energy Storage With Low Temperature Heat Integration," Energy, **145**, pp. 665–676.
[28] Frate, G. F., Antonelli, M., and Desideri, U., 2017, "A Novel Pumped Thermal Electricity Storage (PTES) System With Thermal Integration," Appl. Therm. Eng., **121**, pp. 1051–1058.
[29] Lemmon, E. W., Bell, I. H., Huber, M. L., and McLinden, M. O., 2018, "NIST Standard Reference Database 23: Reference Fluid Thermodynamic and Transport properties-REFPROP, Version 10.0, National Institute of Standards and Technology," Standard Ref. Data Program.
[30] Astolfi, M., Alfani, D., Lasala, S., and Macchi, E., 2018, "Comparison Between ORC and CO2 Power Systems for the Exploitation of Low-Medium Temperature Heat Sources," Energy, **161**, pp. 1250–1261.
[31] SINTEF, 2021, "Developing the World's 'Hottest' Heat Pump Ever," SINTEF, Trondheim, Norway, accessed May 1, 2024, https://www.sintef.no/en/latest-news/2021/developing-the-worlds-hottest-heat-pump-ever/
[32] Gnielinski, V., 1976, "New Equations for Heat and Mass Transfer in Turbulent Pipe and Channel Flow," Int. Chem. Eng., **16**(2), pp. 359–368.
[33] Cavallini, A., Col, D. D., Doretti, L., Matkovic, M., Rossetto, L., Zilio, C., and Censi, G., 2006, "Condensation in Horizontal Smooth Tubes: A New Heat Transfer Model for Heat Exchanger Design," Heat Transfer Eng., **27**(8), pp. 31–38.
[34] Mahir, M., El Maakoul, A., Khay, I., Saadeddine, S., and Bakhouya, M., 2021, "An Investigation of Heat Transfer Performance in an Agitated Vessel," Processes, **9**(3), p. 468.
[35] Liu, Z., and Winterton, R. H. S., 1991, "A General Correlation for Saturated and Subcooled Flow Boiling in Tubes and Annuli, Based on a Nucleate Pool Boiling Equation," Int. J. Heat Mass Transfer, **34**(11), pp. 2759–2766.
[36] Žukauskas, A., 1972, "Heat Transfer From Tubes in Crossflow," *Advances in Heat Transfer*, Academic Press, Cambridge, MA, pp. 93–160.
[37] Cooper, M. G., 1984, "Heat Flow Rates in Saturated Nucleate Pool Boiling-A Wide-Ranging Examination Using Reduced Properties," *Advances in Heat Transfer*, Elsevier, Amsterdam, The Netherlands, Vol. 16, pp. 157–239.
[38] Macchi, E., and Astolfi, M., 2016, *Organic Rankine Cycle (ORC) Power Systems*, Elsevier Science, Amsterdam, The Netherlands.
[39] Lund, H., Østergaard, P. A., Nielsen, T. B., Werner, S., Thorsen, J. E., Gudmundsson, O., Arabkoohsar, A., and Mathiesen, B. V., 2021, "Perspectives on Fourth and Fifth Generation District Heating," Energy, **227**, p. 120520.
[40] Incropera, F. P., DeWitt, D. P., Bergman, T. L., and Lavine, A. S., 2018, *Principles of Heat and Mass Transfer*, John Wiley & Sons, Hoboken, NJ.
[41] National Fire Protection Association, 2017, *NFPA 704, Standard System for the Identification of the Hazards of Materials for Emergency Response*, National Fire Protection Association, Quincy, MA.
[42] Astolfi, M., 2014, "An Innovative Approach for the Techno-Economic Optimization of Organic Rankine Cycles," Ph.D. dissertation, Politecnico di Milano, Italy.
[43] Turton, R., Bailie, R. C., Whiting, W. B., and Shaeiwitz, J. A., 2008, *Analysis, Synthesis and Design of Chemical Processes*, Pearson Education, London, UK.
[44] Loh, H. P., Lyons, J., and White, C. W., 2002, "Process Equipment Cost Estimation, Final Report," *National Energy Technology Lab.(NETL)*, Morgantown, WV.
[45] Perry, G., and Green, D. W., 1997, *Perry's Chemical Engineer's Handbook*, McGraw-Hill, New York.
[46] Quoilin, S., Den Broek, M. V., Declaye, S., Dewallef, P., and Lemort, V., 2013, "Techno-Economic Survey of Organic Rankine Cycle (ORC) Systems," Renewable Sustainable Energy Rev., **22**, pp. 168–186.
[47] International Energy Agency, 2022, "Electricity Market Report," International Energy Agency, Paris, France, accessed May 2, 2024, https://www.iea.org/reports/electricity-market-report-july-2022
[48] Næss-Schmidt, S., Jensen, H. N., and Jasper, L., 2021, "District Heating Tariffs in Europe, Comparison of Tariffs and Regulation in Europe," accessed May 2, 2024, https://open.overheid.nl/repository/ronl-ec66e0006b7e0acc22629091d63-b448a4af5b0c3/1/pdf/heating-tariffs-in-europe.pdf

Downloaded from http://asmedigitalcollection.asme.org/gasturbinespower/article-pdf/146/10/101013/7343132/gtp_146_10_101013.pdf by Politecnico Di Milano user on 09 July 2024